ADVANCES IN ATMOSPHERIC SCIENCES, VOL. 26, NO. 4, 2009, 707–716

The Antarctic Oscillation-East Asian Summer Monsoon Connections in NCEP-1 and ERA-40

ZHU Yali*[1,2,3] (祝亚丽)

[1] *Nansen-Zhu International Research Center, Institute of Atmospheric Physics, Chinese Academy of Sciences, Beijing* 100029

[2] *Graduate University of Chinese Academy of Sciences, Beijing* 100049

[3] *Climate Change Research Center (CCRC), Chinese Academy of Sciences, Beijing* 100029

(Received 6 December 2008; revised 8 January 2009)

ABSTRACT

Connections between the spring Antarctic Oscillation (AAO) and the East Asian summer monsoon (EASM) in two reanalysis datasets—NCEP-1 (NCEP/NCAR Reanalysis 1) and ERA-40 (ECMWF 40-year Reanalysis)—are investigated in this study. Both show significant correlation between AAO and EASM rainfall over the Yangtze River valley, especially after about 1985. Though ERA-40 shows weaker anomalous signals connecting AAO and EASM over southern high latitudes than NCEP-1, both datasets reveal similar connecting patterns between them. A wave-train-like pattern appears in the upper levels, from southern high latitudes through east of Australia and from the Maritime Continent to East Asia. In positive AAO years, the cross equatorial southeasterly flow over the Maritime Continent in the lower levels is strengthened, the specific humidity of the whole atmosphere over East Asia increases, and convective activity is enhanced; thus the summer rainfall over East Asia increases. The spring AAO-EASM connection may be better represented in ERA-40.

Key words: Antarctic Oscillation, East Asian summer monsoon, NCEP-1, ERA-40

Citation: Zhu, Y. L., 2009: The Antarctic oscillation-East Asian summer monsoon connections in NCEP-1 and ERA-40. *Adv. Atmos. Sci.*, **26**(4), 707–716, doi: 10.1007/s00376-009-8196-2.

1. Introduction

The East Asian summer monsoon (EASM), which dominates China, Korea, and Japan, is an important component of the summer monsoon system, and is closely related to the summer precipitation in East Asia. Thus, a large proportion of the rainfall variability in East Asia emanates from the variation of EASM. The interannual variability of EASM comes from several sources, such as the remote and local sea surface temperature, land surface processes including snow/ice cover, soil moisture, broad scale atmospheric circulation, and so on (Wang, 2006). Atmospheric circulation influencing the intensity of EASM includes the western Pacific subtropical high (Huang and Sun, 1994; Sun and Ma, 2001), the Middle East jet stream, the East Asian jet stream, the Arctic Oscillation, as well as the Southern Hemispheric circulation, as addressed by many papers in recent years. Studies on the possible link between the Southern Hemispheric circulation and East Asian climate started many years ago, and have been revived lately especially by meteorologists in East Asia.

Krishnamurti (1979) studied the Asian monsoon system, including the connection between EASM and the Mascarene high (MH) and the related Somali jet, and Tao and Chen (1987) addressed another system covering the connection between the Australian high (AH) and the related cross-equatorial flow. Recently, following the further understanding of the major modes in high-latitude atmospheric circulation (Gong and Wang, 1999; Thompson and Wallace, 2000), more studies concerning the cross-equatorial influence of the atmospheric systems in southern high

*Corresponding author: ZHU Yali, zhuyl@mail.iap.ac.cn

latitudes have been performed. Xue et al. (2003, 2004) investigated the detailed influence of the MH and the Antarctic Oscillation (AAO) on EASM circulation and summer rainfall in the Yangtze River valley using NCEP-1 (the National Centers for Environmental Prediction/National Centers for Atmospheric Research Renalysis 1, Kalnay et al., 1996) and model ensemble simulations. Nan and Li (2003) further substantiated the positive correlation between the southern annular mode (also named Antarctic Oscillation) and summer precipitation in the middle and lower reaches of the Yangtze River valley. Fan and Wang (2004, 2006) showed a negative correlation between spring dust weather frequency in northern China and the winter-spring Antarctic Oscillation. Wang and Fan (2005) explored the manifestation of AAO signal in the circulation fields associated with the central-north China precipitation, and obtained a significant negative correlation between the AAO and the precipitation time series reconstructed from Qing Dynasty historical documents. The AAO is also identified to be associated with tropical cyclone activity in the western North Pacific (Wang and Fan, 2007).

Reanalysis data are irreplaceable in such long-term, large-scale diagnostic studies. So far, there are two alternative sources of reanalyses, including the above mentioned NCEP-1 with a period from January 1948 to near-present and the ERA-40 (ECMWF 40-year Reanalysis) from September 1958 to August 2002 produced at the European Centre for Medium-Range Weather Forecast (Uppala et al., 2004). Despite the wide use of both reanalyses, their credibility is still to be validated because of their dependence on both observing systems and forecast models. From this point of view, comparisons between the two reanalyses as well as between reanalyses and available observational datasets are still necessary and effective ways to help better interpret and understand the results gained by analyzing the reanalyses, although previous comparison studies have not always provided consistent conclusions so far about the quality of the reanalyses. Pawson and Fiorino (1998) contrasted the observations and atmospheric general circulation models used in the two reanalyses. Sterl (2004) compared the two reanalyses and revealed many inhomogenities, mainly in the Southern Hemisphere and before 1980. Trenberth et al. (2001) made a comparison between a somewhat independent observational temperature product from the microwave sounder unit and the two reanalyses, and found fairly good agreement overall for NCEP-1, and large discrepancies with ERA-15 (ECMWF 15-year reanalysis), especially in the tropics. Several studies have investigated the performance of the reanalyses in Asia. Annamalai et al. (1999) compared ERA-15 and NCEP-1 for the mean evolution and variation of the Asian summer monsoon, and part of their conclusions were that: ERA-15 is suggested to provide a more reliable description of the seasonal mean monsoon, but there is little evidence to suggest that one reanalysis is superior to the other in terms of interannual variability. Zhao and Fu (2006) found that the Climate Research Unit TS 2.1 precipitation dataset best matches the observed summer precipitation, while ERA-40 reports less precipitation and NCEP-2 (NCEP/NCAR version 2) reports more than the observations.

All these previous comparison studies reveal large discrepancies as well as consistencies among different reanalyses. Therefore, to test the credibility of the possible link between Antarctic Oscillation and EASM and to obtain more reliable results that can be used in the operational forecast, it is necessary to analyze ERA-40 data as well, since all previous studies on the linkage was performed by using the NCEP reanalysis alone. The data employed in this study is introduced briefly in section 2, and the results are shown in section 3. Section 4 presents suggestions and conclusions based on the results.

2. Datasets

The geopotential height, wind field, outgoing longwave radiation (OLR), and specific humidity in two reanalyses, NCEP-1 and ERA-40, are employed. Another source of OLR data is derived from the National Oceanic and Atmospheric Administration (NOAA) directly, which is interpolated based on satellite observations, except for 17 March to 31 December of 1978, which is unavailable due to satellite failure. The 160-station based observational precipitation in China is obtained from the website of the China Meteorological Administration data archives, and is widely used by meteorologists to study East Asian climate. The 160 stations are not uniformly distributed, but rather have dense clustering over eastern China and sparse coverage over the western part, still basically satisfying our needs for this study. The station data is interpolated onto a $1^\circ \times 1^\circ$ grid.

The AAO index is computed as the leading empirical orthogonal function (EOF-1) of the 850 hPa geopotential height south of 20°S. The El Niño-Southern Oscillation index is measured by the three-month running mean of sea surface temperature anomalies in the Niño 3.4 region, which can be downloaded from http://www.cpc.ncep.noaa.gov/.

3. Results

Figure 1 shows the difference between the climatological summer mean (June–July–August) state, geo-

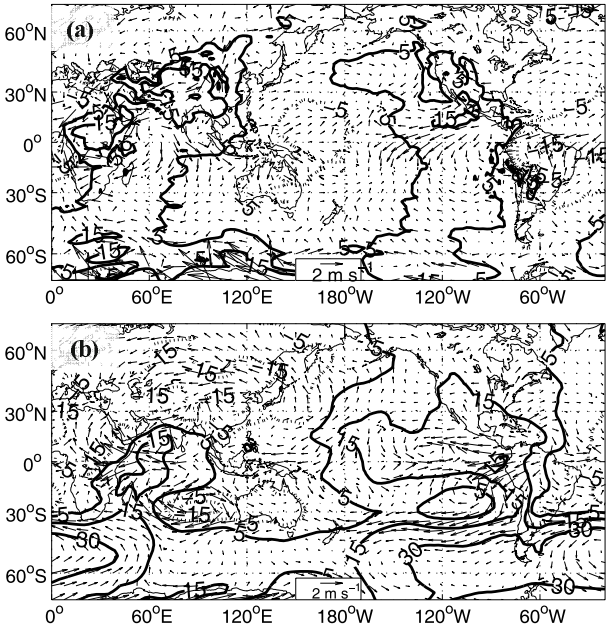

Fig. 1. The difference between climatological summer mean (June–July–August) state of geopotential height (contours), and wind (vectors) at (a) 850 hPa and (b) 200 hPa during 1971–2000 in NCEP-1 and ERA-40. Contour values are −15, −5, 5, 15, and 30 gpm (geopotential height meter), dashed lines indicate negative values.

potential height (contours), and wind (vectors) at 850 hPa and 200 hPa levels during 1971–2000 in NCEP-1 and ERA-40. At low levels, large discrepancies occur over the western tropical and eastern Pacific, Africa, and the Indian Ocean. The centers over the Tibetan Plateau (Zhao et al., 2008) and Antarctica are unrealistic because the equivalent height of 850 hPa is underground in these areas. At the upper levels, inconsistency between reanalyses also appears over the above locations except for the two unrealistic centers. NCEP-1 shows higher geopotential height values over most of the region south of 30°S, the Indian Ocean, the eastern tropical Pacific, and southern North America; NCEP-1 shows lower values over most of Asia. All these features reveal a significant difference between NCEP-1 and ERA-40, and thus show the necessity of making a specific contrast between NCEP-1 and ERA-40 in terms of the linkage between AAO and EASM.

Previous studies (Sterl, 2004) have presented that the largest inconsistency between the two reanalyses exists before 1980. Here, we first correlate AAO and the station rainfall during the period 1970–2002 (Figs. 2a and 2b), which was selected based on a compromise between two considerations: (1) changes in the observing system, specifically the introduction of satellite data into reanalyses during the late 1970s, have some impacts on the quality of the two reanalyses,

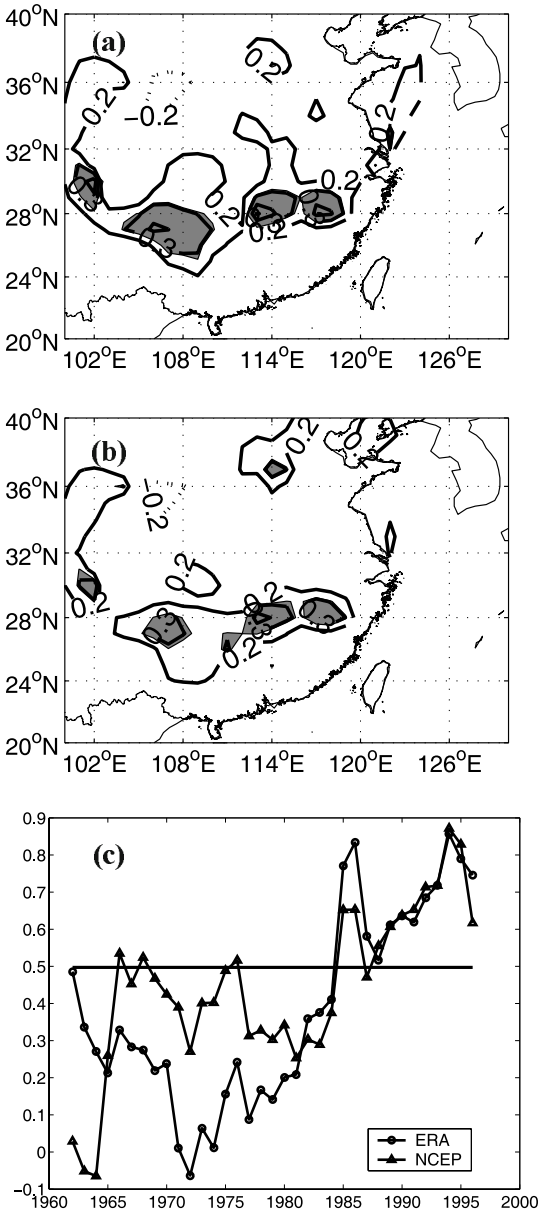

Fig. 2. The correlation map between summer 160-station rainfall in China and the preceding spring AAO in (a) NCEP-1, and (b) ERA-40 during 1970–2002, shadings in (a) and (b) indicate significant areas above 10% level; (c) the running correlation with a 11-year window, between AAO and the rainfall index for NCEP-1 (solid-triangle line) and ERA-40 (solid-circle line).

and thus the common period 1958–2002 may include some pseudo-signals; (2) statistically, longer data is often better for studying the possible linkage between two or more climatic systems. Significant correlation coefficients appear over mid-southern China in both panels, only with larger scale and higher values in NCEP-1. Then, to obtain an idea about the correla-

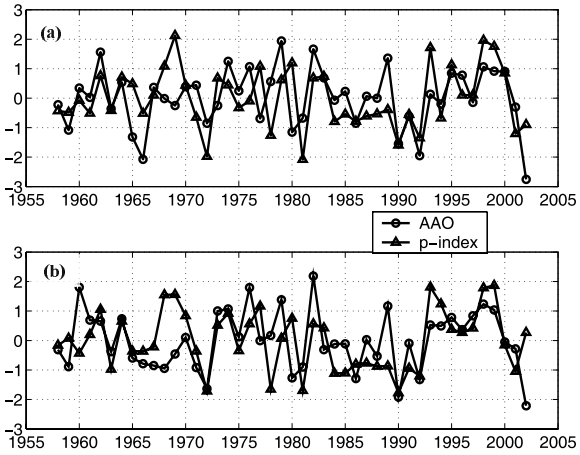

Fig. 3. Detrended and standardized AAO index (circle markers) in (a) NCEP-1, and (b) ERA-40, and the rainfall index (triangle markers) during 1958–2002.

tion between AAO and the regional rainfall, a rainfall index is defined as the mean precipitation of the stations with correlation coefficients (between AAO index and station rainfall) higher than 0.2 in the domain of 24°–32°N, east of 103°E in Figs. 2a and 2b for the two reanalyses, respectively. The correlation coefficients between the original AAO in NCEP-1/ERA-40 and the rainfall indices are 0.52/0.49 during 1970–2002, and 0.44/0.52 after detrending. This contrast is probably attributed to the somewhat exaggerated trend of AAO in NCEP-1 (with a trend of 3.04 and 0.46 for the standardized spring AAO index in NCEP-1 and ERA-40 during 1970–2002), which has been pointed out by many previous studies (Marshall, 2003).

In order to study the variation of the connection, we simply perform a running correlation with the AAO and the original rainfall index during 1950–2002 using an 11-year window (Fig. 2c). The trend of both indices is removed before this computation. Figure 2c reveals the unstable connection between the AAO and the rainfall index in both datasets: the correlation coefficient is not significant until the mid-1980s. The detrended and normalized indices are shown in Fig. 3. Both AAO indices in ERA-40 and NCEP-1 show an in-phase co-variation with the original rainfall index after about 1985, while no obvious co-variation occuring during the preceding period. Thus, we select 1985–2002 as the period of interest in the following analyses.

The correlation maps between AAO and station rainfall during 1985–2002 are presented in Figs. 4a and 4b, showing a highly consistent pattern in NCEP-1 and ERA-40. The significant areas in Figs. 4a and 4b have become much larger than in Figs. 2a and 2b, implying the adequateness of selecting this period. We also examine the correlation between ENSO and EASM rainfall, and find that the ENSO signal in the preceding winter can influence the summer rainfall, but the impact is only significant over a very small area (as shown in Fig. 4c). However, in consideration of the potential influence of ENSO on the linkage between AAO and EASM, the linear signal of preceding winter ENSO is removed from all the indices and fields. A new rainfall index is defined as the mean precipitation of all the stations in the domain of 26°–32°N, 108°–120°E according to Figs. 4a and 4b, as almost the whole area is occupied by significant correlation coefficients. Figure 4d shows the three indices during 1985–2002: the spring AAO in NCEP-1 and ERA-40 (with a correlation coefficient of 0.94 between them), and the summer rainfall index (all the three indices detrended, ENSO signals linearly removed, and standardized). Both AAO indices show an in-phase covariation with the rainfall index. The correlation coefficient between the original AAO in NCEP-1/ERA-40 and the rainfall index is 0.61/0.53 and 0.53/0.54 after detrending (with a trend of 1.78/1.04 for the AAO in NCEP-1/ERA-40 during 1985–2002), and 0.58/0.60 after the ENSO signal is removed; all results are significant with above 95% confidence level via student t-test. The above statistics manifest again the impact of the AAO trend on this correlation, the subtle influence of ENSO, and the robustness of the correlation between the AAO and the EASM regional rainfall.

All the above analyses show the significant correlation between the spring AAO and the EASM rainfall over mid-southern China in both reanalyses, especially during 1985–2002. The similarities and differences between the detailed linkages in NCEP-1 and ERA-40 will be discussed specifically as follows.

Following a positive spring AAO, the summer 850-hPa geopotential height field (Figs. 5a and 5b) is occupied with negative anomalies in the southern high latitudes, centered at about 65°S, 140°W; there are positive anomalies in the southern middle latitudes, with two small centers inhabiting the ocean south of Australia and the middle south Pacific. These positive anomalies even expand across the equatorial Pacific into East Asia. NCEP-1 shows a much more robust negative center in the southern high latitudes and a larger significant area in the eastern equatorial Pacific, while the positive center over the southern middle latitudes appears somewhat stronger in ERA-40. ERA-40 also depicts somewhat larger-scale significant positive anomalies occupying East Asia, which is more significant at the upper levels (not shown). A similar spatial pattern is also obtained by regression against the rainfall index (Figs. 5c and 5d). This method shows the negative center to be located more northeastward at

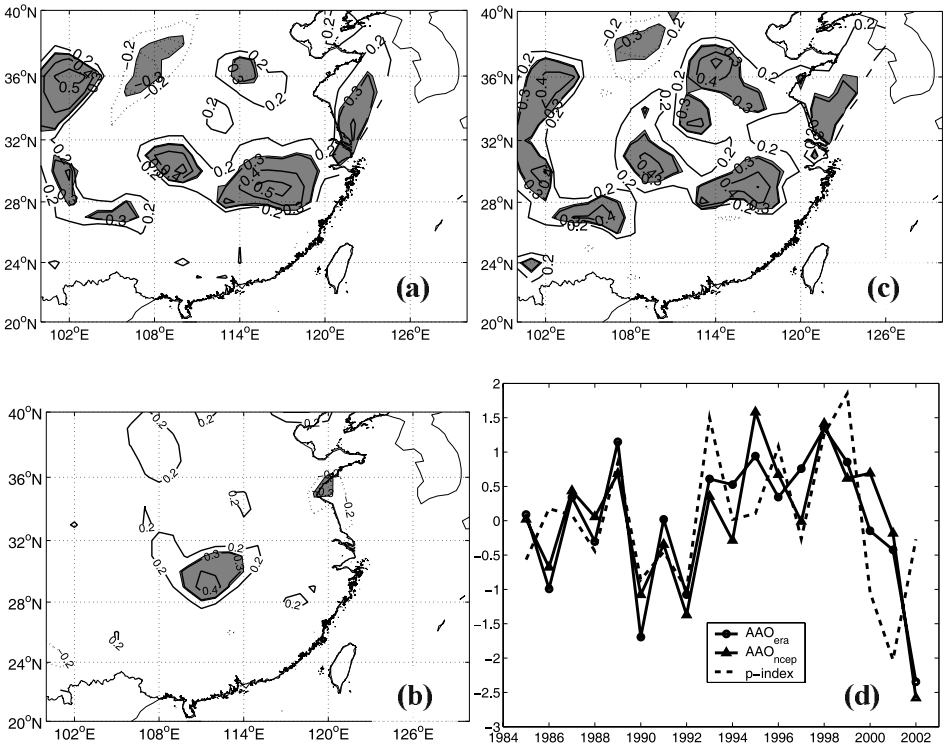

Fig. 4. The correlation map between summer 160-station rainfall in China and preceding spring AAO in (a) NCEP-1, (b) ERA-40, and also with (c) the preceding winter Niño 3.4 index during 1985–2002. (d) shows the detrended, ENSO-removed, standardized indices during 1985–2002; solid-circle, solid-triangle, and dashed lines represent AAO in ERA-40, AAO in NCEP-1, and the rainfall index, respectively, with shading as in Fig. 2a.

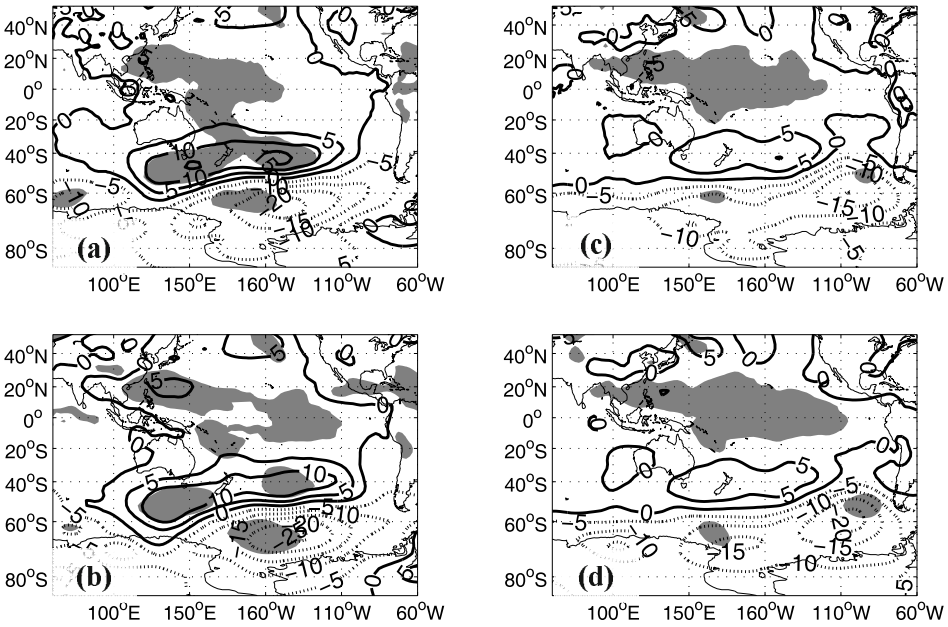

Fig. 5. The regressed summer 850-hPa geopotential height field during 1985–2002 in (a) NCEP-1 and (b) ERA-40, both against spring AAO; (c) NCEP-1 and (d) ERA-40 regressed against the summer rainfall index. Shading indicates significant areas above 95% level. Units: gpm std^{-1}.

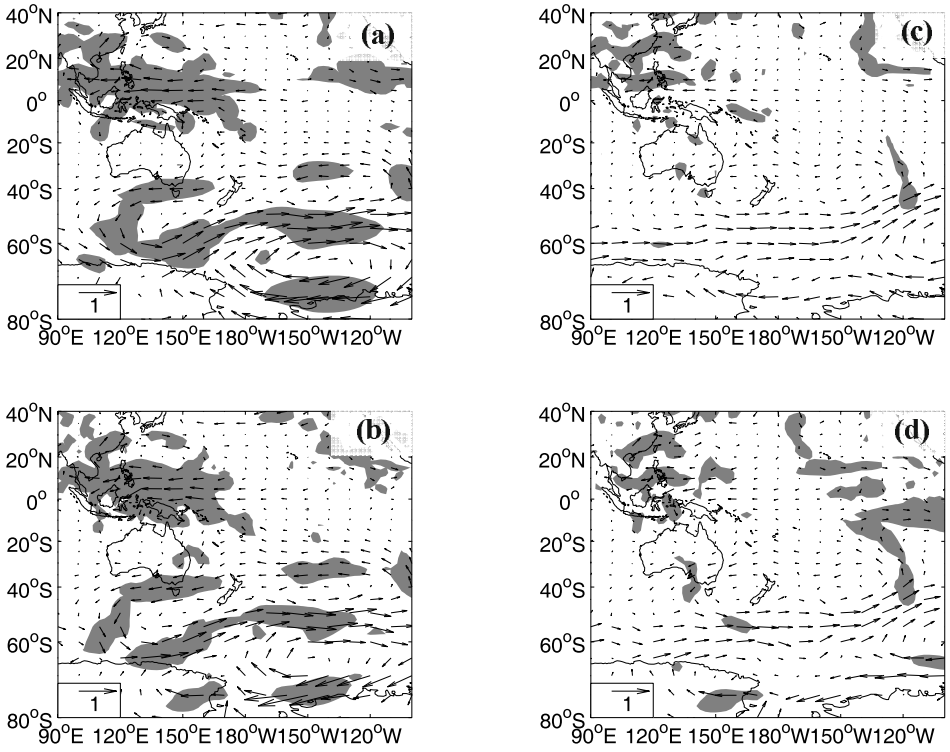

Fig. 6. As in Fig. 5, but for the 850-hPa wind field. Units: m s^{-1} std^{-1}.

about 110°W, 60°S, and there is less robustness of the Southern Hemisphere anomaly centers, but a larger significant area deep into South and East Asia.

Correspondingly, significant cyclonic and anticyclonic anomalies appear over southern high and middle latitudes following a positive spring AAO event (Figs. 6a and 6b). The anomalous southeasterly outflow from the anticyclonic anomalies in the southern middle latitudes strengthens the cross-equatorial flow over the western Pacific, and enhances the easterly flow near the equator over the Maritime Continent. Part of the easterly flow curls anticyclonically to the north, and thus the anomalous southerly flow from the ocean to East Asia is intensified. In the regressions onto the rainfall index (Figs. 6c and 6d), the westerly flow near 60°S is also strengthened. The enhanced easterly flow over the Maritime Continent and the anticyclonic anomalies with southerly anomalies flowing toward East Asia favor a strengthened summer monsoon.

At the upper levels (Fig. 7), a wave-train-like pattern, with alternating cyclonic and anticyclonic anomalous centers from southern high latitudes from the Maritime Continent to East Asia, can be observed in the regression field onto either AAO or the rainfall index. This wave-train-like pattern is somewhat different from the Pacific-Japan (PJ) teleconnection pattern pointed out by Nitta (1987), and the teleconnection pattern of Xue et al. (2003). The anomalous southwesterly flow over the Maritime Continent in Figs. 7a and 7b is closely linked with the large scale cyclonic anomalies spanning over the middle subtropical Indian Ocean to the east of Australia. In Figs. 7c and 7d, this anomalous cyclone locates more eastward to the east coast of Australia. The westerly anomalies at the upper levels over the Maritime Continent can reduce the climatological mean weak easterly wind, and even turn it to westerly, and then the wave-train-like pattern in Fig. 7 can penetrate through the equator and propagate into East Asia. Thus, the AAO probably exerts impact on EASM mainly through a narrower wave-train-like passage via the area east of Australia and the Maritime Continent. Again, NCEP-1 shows more robust anomalous signals, especially in the Southern Hemisphere.

In addition to the large scale anomalous atmospheric circulation, water content in the atmosphere is another important factor influencing regional rainfall. Figure 8 shows the regressed total specific humidity between 300 hPa and 1000 hPa. In positive AAO years, the specific humidity is increased over southern China, southern Japan, and the Maritime Continent, and decreased over the Western Pacific. Increased moisture in the air favors increased EASM regional rainfall. Another obvious feature is that positive anomalies appear over the Tibetan Plateau in

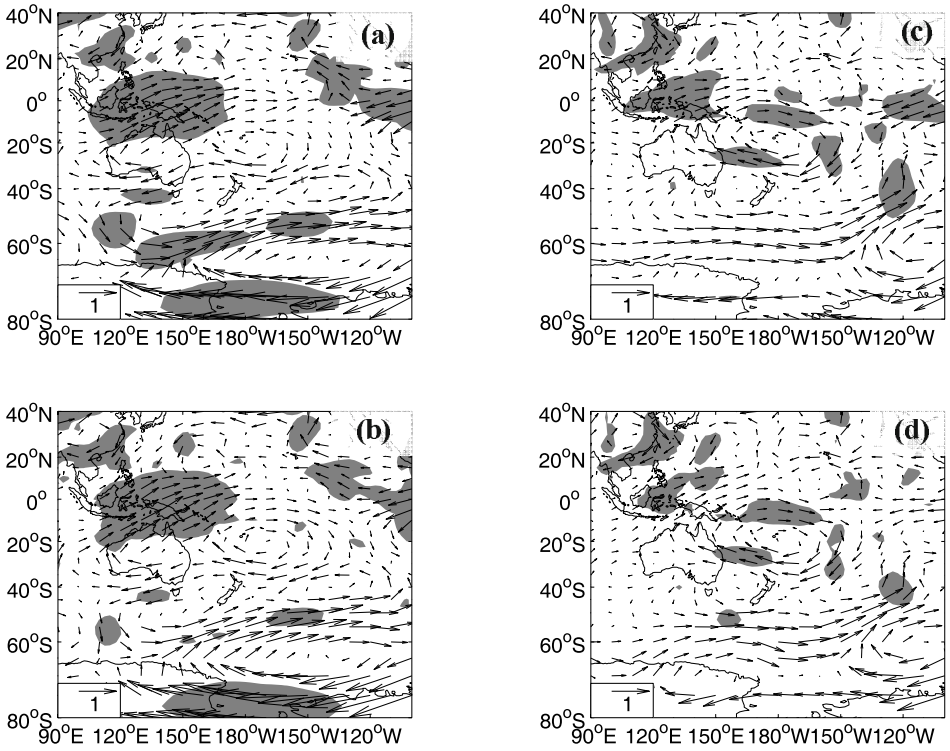

Fig. 7. As in Fig. 5, but for the 200 hPa wind field. Units: m s^{-1} std^{-1}.

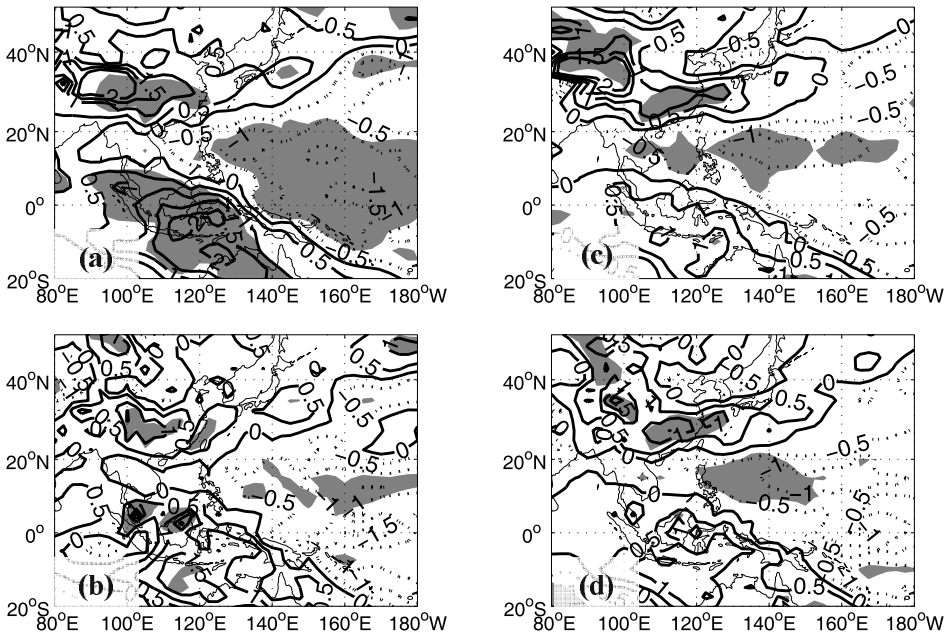

Fig. 8. As in Fig. 4, but for total specific humidity between 300 hPa and 1000 hPa. Contour interval is 0.5. Units: g kg^{-1} std^{-1}.

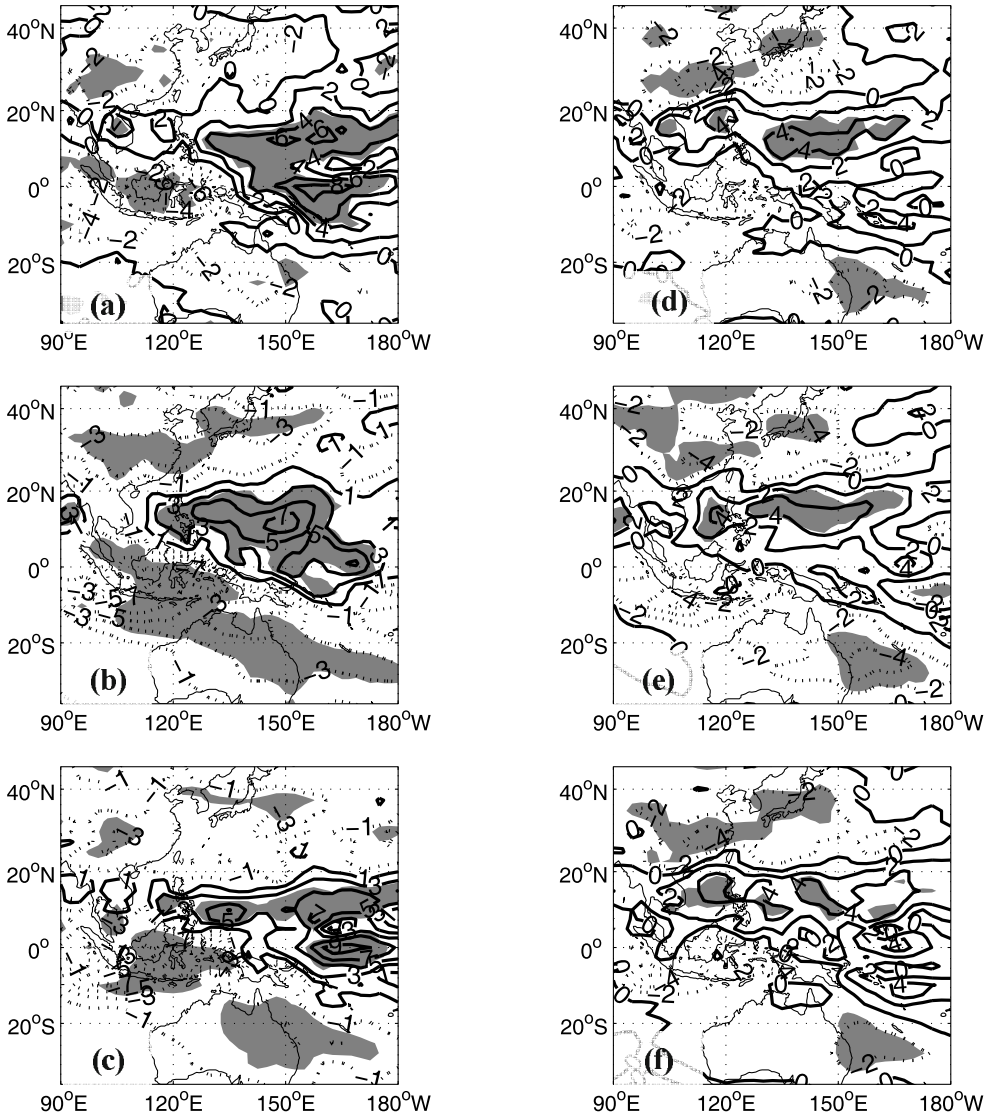

Fig. 9. The regressed outgoing long-wave radiation during 1985–2002 in (a) NOAA data against the spring AAO in NCEP-1; (b) NCEP-1 OLR against spring AAO; (c) ERA-40 against spring AAO; (d), (e), (f) are the same as (a), (b), (c), but against the summer rainfall index. Contour interval is 2. Units: W m^{-2} std^{-1}.

both NCEP-1 and ERA-40, but with much stronger positive anomalies in NCEP-1. This can probably be attributed to the biases closely related to the local topography, because "spurious" moisture exists over the Plateau. The negative anomalies over the western tropical Pacific are also much more stronger in NCEP-1 than in ERA-40.

The outgoing long-wave radiation data of NOAA is derived from satellite data, and can be treated as an objective reference to evaluate the outgoing long-wave radiation field in the reanalyses. In positive AAO years, both reanalyses (Figs. 9b and 9c) show similar anomalous centers compared to NOAA data (Fig. 9a): significant negative anomalies appear east of Australia, over the Maritime Continent, and over southern East Asia (including southern China and southern Japan), representing enhanced convective activity over these regions. Significant positive anomalies over the western and middle tropical Pacific indicate depressed convective activity. Regressions against the rainfall index (Figs. 9d, 9e and 9f) show there are significant negative-positive-negative centers east of Australia, in the northwestern tropical Pacific, and over East Asia. Despite the overall similar pattern in both reanalyses with NOAA data, NCEP-1 shows stronger and larger anomalous centers, especially over western Pacific and East Asia, while ERA-40 has somewhat more similarity with NOAA in terms of the magnitude and scale

of the anomalies.

4. Discussions and conclusions

The purpose of this paper is to compare the association between spring AAO and EASM rainfall in two available reanalyses—NCEP-1 and ERA-40. Mechanisms in connecting them are not developed very deeply in this study, and can be referred to in previous researches (e.g., Xue et al., 2003; Nan and Li, 2003). Recently, Sun et al. (2008) discusses the possible mechanism linking the spring AAO and EASM rainfall in detail, and reveal that the convection activity over the region of the Maritime Continent serves as a bridge in this connection.

We first define an original rainfall index according to the correlation map between AAO and 160-station rainfall during 1970–2002. The running correlation in both datasets shows the significant connection between the AAO and the original EASM rainfall index after the 1980s. The correlation pattern between the AAO and station rainfall during 1985–2002 reveals significant correlation in the domain of 26°–32°N, 108°–120°E. And the mean rainfall over this area is defined as the new EASM rainfall index. All the analyzed fields are detrended and subtracted by the linear signal of the preceding winter ENSO in subsequent calculations.

Though NCEP-1 shows much stronger significant anomalies over the southern high latitudes than ERA-40, both reanalyses reveal similar pattern linking AAO and EASM. The most significant linkage between AAO and EASM circulation appears at upper levels in both reanalyses.

In the regressed summer 200 hPa wind field, the spring AAO variability is linked to a wave-train-like pattern with alternating cyclonic and anticyclonic anomalies from the southern high latitudes through east of Australia and the Maritime Continent to East Asia, and anomalous northerly winds dominate East Asia. The summer rainfall index is also related with a similar pattern, only with weaker centers in southern high latitudes. At the low levels, the anomalous cross-equatorial southerly flow over the western tropical Pacific and the anomalous easterly winds over the Maritime Continent are enhanced in positive AAO years, with anomalous southerly winds diverging from the latter current laden with moisture from the western Pacific to East Asia. Dry summers are often accompanied by weaker cross-equatorial flow over the western tropical Pacific.

The AAO (positive) index is also significantly related to the water content in a manner suggesting increased total specific humidity over the Maritime Continent and East Asia, and decreased humidity over the western Pacific. Positive spring AAO events are often followed by increased convective activity east of Australia, over the Maritime Continent, and in East Asia, and depressed convective activity over the southwestern tropical Pacific. Dry years in East Asia are often linked with anomalous downward motion east of Australia and over East Asia, and anomalous upward motion over the southwestern tropical Pacific. Generally, NCEP-1 shows larger anomalous centers, while ERA-40 exhibits a more consistent pattern of anomalies with NOAA OLR.

Acknowledgements. The authors would like to thank Dr. A. Grinsted for providing the wavelet analyses programs. This research was jointly supported by National Basic Research Program of China (973 Program) under Grant No. 2009CB421406, the Chinese Academy of Sciences under Grant KZCX2-YW-Q1-02, and the National Natural Science Foundation of China under Grants Nos. 40875048, 40620130113, and 40631005.

REFERENCES

Annamalai, H., J. M. Slingo, K. R. Sperber, and K. Hodges, 1999: The mean evolution and variability of the Asian summer monsoon: Comparison of ECMWF and NCEP-NCAR reanalyses. *Mon. Wea. Rev.*, **127**, 1157–1186.

Fan, K., and H. J. Wang, 2004: Antarctic oscillation and the dust weather frequency in North China. *Geophys. Res. Lett.*, **31**, L10201.

Fan, K., and H. J. Wang, 2006: Interannual variability of Antarctic Oscillation and its influence on East Asian climate during boreal winter and spring. *Science in China*(*D*), **49**(5), 554–560.

Gong, D. Y., and S. W. Wang, 1999: Definition of Antarctic Oscillation Index. *Geophys. Res. Lett.*, **26**, 459–462.

Huang, R. H., and F. Y. Sun, 1994: The impact of thermal state in the western Pacific warm pool and the convective activity above the warm pool on the East Asian climate anomalies. *Chinese J. Atmos. Sci.*, **18**, 141–151. (in Chinese)

Kalnay, E., and Coauthors, 1996: The NCEP/NCAR 40-Year Reanalysis Project. *Bull. Amer. Meteor. Soc.*, **77**, 437–471.

Krishnamurti, T. N., 1979: Tropical meteorology. *Compendium of Meteorology*, A. Wan-Nielsen, Ed., WMO No. 364, 428pp.

Marshall, G. J., 2003: Trends in the Southern annular mode from observations and reanalyses. *J. Climate*, **16**, 4134–4143.

Nan, S. L., and J. P. Li, 2003: The relationship between the summer precipitation in the Yangtze River valley and the boreal spring Southern Hemisphere annular mode. *Geophys. Res. Lett.*, **30**, 2266.

Nitta, T., 1987: Convective activities in the tropical western Pacific and their impact on the northern hemisphere summer circulation. *J. Meteor. Soc. Japan*, **65**, 373–390.

Pawson, S., and M. Fiorino, 1998: A comparison of reanalyses in the tropical stratosphere. Part 2: The quasi-biennial oscillation. *Climate Dyn.*, **14**, 645–658.

Sterl, A., 2004: On the (in) homogeneity of reanalysis products. *J. Climate*, **17**, 3866–3873.

Sun, J. Q., H. J. Wang, and W. Yuan, 2008: A possible mechanism for the co-variability of the boreal spring Antarctic Oscillation and the Yangtze River valley summer rainfall. *International Journal of Climatology*, doi: 10.1002/joc.1773.

Sun, S. Q., and S. J. Ma, 2001: Anomalies of the western Pacific subtropical high and its relation to the flood in Yangtze River Valley in 1998. *Acta Meteorologica Sinica*, **59**, 719–729. (in Chinese)

Tao, S. Y., and L. X. Chen, 1987: the East Asian summer. *Review in Monsoon Meteorology.*, Oxford University Press, 60–92.

Thompson, D. W. J., and J. M. Wallace, 2000: Annular modes in the extratropical circulation. Part I: Month-to-month variability. *J. Climate*, **13**, 1000–1016.

Trenberth, K. E., D. P. Stepaniak, J. W. Hurrell, and M. Fiorino, 2001: Quality of reanalyses in the Tropics. *J. Climate*, **14**, 1499–1510.

Uppala, S., and Coauthors, 2004: ERA-40: ECMWF 45-year reanalysis of the global atmosphere and surface conditions 1957–2002. *ECMWF Newsletter Meteorology*, **101**, 2–21.

Wang, B., 2006: *The Asian Monsoon*. Springer, in association with Praxis Publishing, 268–279.

Wang, H. J., and K. Fan, 2005: Central-north China precipitation as reconstructed from the Qing dynasty: Signal of the Antarctic Atmospheric Oscillation. *Geophys. Res. Lett.*, **32**, L24705.

Wang, H. J., and K. Fan, 2007: Relationship between the Antarctic oscillation and the western North Pacific typhoon frequency. *Chinese Science Bulletin*, **52**(4), 561–565.

Xue, F., H. J. Wang, and J. H. He, 2004: Interannual variability of Mascarene High and Australian High and their influences on East Asian summer monsoon. *J. Meteor. Soc. Japan*, **82**, 1173–1186.

Xue, F., D. B. Jiang, X. M. Lang, and H. J. Wang, 2003: Influence of the Mascarene high and Australian high on the summer monsoon in East Asia: Ensemble simulation. *Adv. Atmos. Sci.*, **20**, 799–809.

Zhao, T. B., and C. B. Fu, 2006: Comparison of products from ERA-40, NCEP-2, and CRU with station data for summer precipitation over China. *Adv. Atmos. Sci.*, **23**, 593–604, doi: 10.1007/s00376-006-0593-1.

Zhao, T. B., W. D. Guo, and C. B. Fu, 2008: Calibrating and evaluating reanalysis surface temperature error by topographic correction. *J. Climate*, **21**, 1440–1446.